

# “Search for the resonance absorption of solar axions emitted in the M1 transition of $^{83}\text{Kr}$ and $^{57}\text{Fe}$ nuclei in the Sun”

Z.A. Akhmatov<sup>5</sup>, S.S. Berezin<sup>4</sup>, Yu.M. Gavriilyuk<sup>1</sup>, A.M. Gangapshev<sup>1</sup>, A.V. Derbin<sup>3</sup>,  
I.S. Drachnev<sup>3</sup>, V.V. Kazalov<sup>1</sup>, A.Kh.-A. Khokonov<sup>5</sup>, V.V. Kuzminov<sup>1</sup>, V.N. Muratova,  
S.I. Panasenko<sup>2</sup>, S.S. Ratkevich<sup>2</sup>, D.A. Tekueva<sup>1</sup>, S.P. Yakimenko<sup>1</sup>,  
E.V. Unzhakov<sup>3</sup>, A.Yu. Zavrazhnov<sup>4</sup>.

<sup>1</sup> – Institute for Nuclear Research RAS, Moscow, Russia

<sup>2</sup> – Kharkov National University, Ukraine

<sup>3</sup> – St. Petersburg Nuclear Physics Inst., NRCKI, Gatchina, Russia

<sup>4</sup> – Voronezh state university, Voronezh, Russia

<sup>5</sup> – Kabardino-Balkarian state university, Nalchik, Russia

*Work is supported by RFBR: 14-02-00258 and 16-29-13011*



“Axions are among the most fascinating particles on the long list of those proposed but not yet observed or ruled out. Their existence would provide an elegant resolution of the strong CP problem. Even more exciting is the possibility that the missing mass needed to close the universe is composed of axions, and that axions are «cold dark matter» which seems to be necessary for galaxy formation. ...”

Mark Srednicki, “Axion couplings to matter (I). CP-conserving parts”, Nucl. Phys. B260 (1985) 689-700.

“...the composite axion is a particular example of a “hadronic” axion, resulting from a theory where only exotic fermions carry  $U(1)_{PQ}$  charges. **Hadronic axions don't couple to leptons**, which are neutral under  $SU(3) \times U(1)_{PQ}$ . Nor do they couple to heavy quarks, which are integrated out of the theory above 1 GeV, where QCD gets strong. **Hadronic axions will still couple to nucleons as well as to photons**. ...”

David B. Kaplan, “Opening the axion window”, Nucl. Phys. B260 (1985) 215-226.

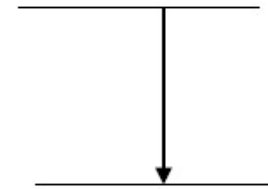
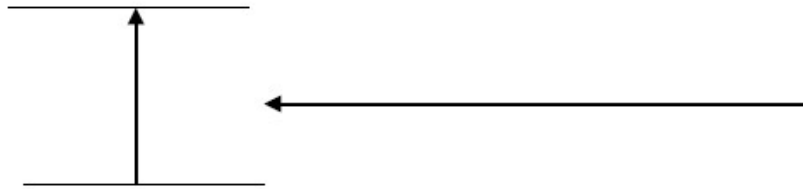
“The most attractive solution of the strong CP problem is to introduce the Peccei-Quinn global symmetry which is spontaneously broken at energy scale  $f_a$ . The original axion model assumed that  $f_a$  is equal to the electroweak scale. Although it has been experimentally excluded, variant “invisible” axion models are still viable in which  $f_a$  is assumed to be very large. ... Such models are referred to as hadronic and Dine-Fischler-Srednicki-Zhitnitskii axions. ....”

Shigetaka Moriyama, “Proposal to search for a monochromatic component of solar axions using  $^{57}\text{Fe}$ ”, Phys. Rev. Lett. v.75 №8 (1995) 3222-3225.

The axions can be produced when thermally excited nuclei (or excited due to nuclear reactions) in the Sun relaxes by magnetic transition to its ground state and could be detected via resonant excitation of the same nuclide in a laboratory.



${}^7\text{Li}$ ,  ${}^{57}\text{Fe}$ ,  ${}^{83}\text{Kr}$   
 ${}^{169}\text{Tm}$



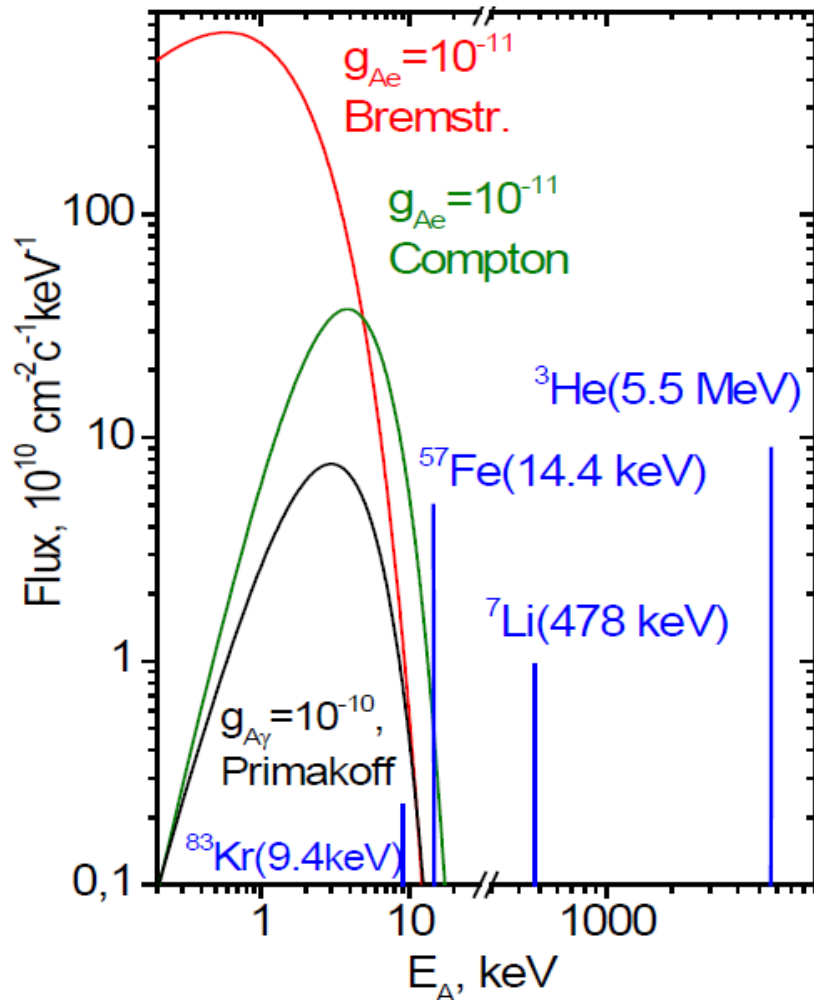
${}^7\text{Li}$ ,  ${}^{57}\text{Fe}$ ,  ${}^{83}\text{Kr}$

Primakoff, Compton and Bremsstrahlung



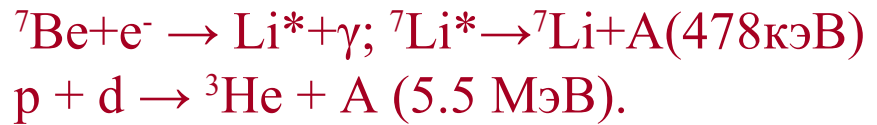
The monochromatic axions emitted by  ${}^7\text{Li}$ ,  ${}^{57}\text{Fe}$  and  ${}^{83}\text{Kr}$  nuclei can excite the same nuclide in a laboratory, because the axions are Doppler broadened due to thermal motion of the axion emitter in the Sun, and thus some axions have needed energy to excite the nuclide.

# Solar axions spectra vs $g_{A\gamma}$ , $g_{Ae}$ and $g_{AN}$



The main sources of solar axions:

1. Reactions of main solar chain. The most intensive fluxes are expected from M1-transitions in  $^7\text{Li}$  and  $^3\text{He}$  nuclei ( $g_{AN}$ ):



2. Magnetic type transitions in nuclei whose low-lying levels are excited due to high temperature in the Sun ( $^{57}\text{Fe}$ ,  $^{83}\text{Kr}$ ) ( $g_{AN}$ )

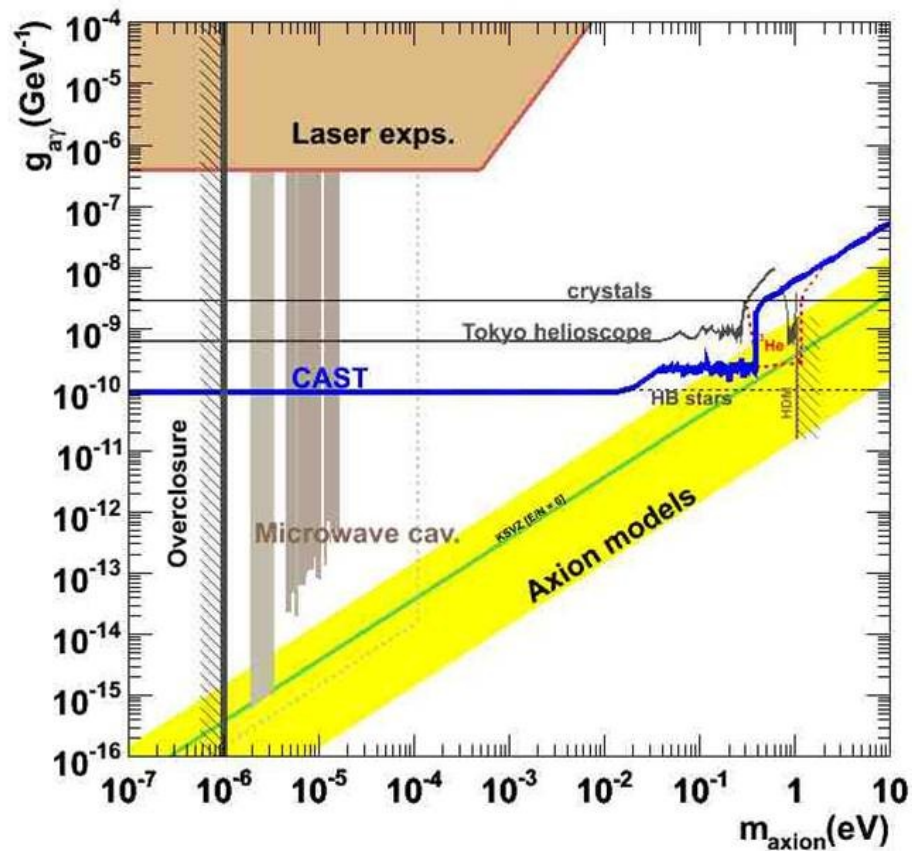
3. Primakoff conversion of photons in the electric field of solar plasma ( $g_{A\gamma}$ ).

4. Bremsstrahlung:  $e + Z(e) \rightarrow Z + A$ . ( $g_{Ae}$ )

5. Compton process:  $\gamma + e \rightarrow e + A$ . ( $g_{Ae}$ )

6. axio-recombination:  $e + I \rightarrow I^- + A$  and axio-deexcitation:  $I^* \rightarrow I + A$ . PRD 83

023505 (2011) CAST 1302.6283, 1310.0823



Limits of the photon-axion coupling constant as a function of the axion mass. The yellow band shows the region favoured by axion models. The blue line represents the lower limit of the region excluded by the data obtained in the first phase of the CAST experiment and the data with 4He, exceeding the limit obtained by stellar constraints. The regions excluded by laser experiments are also shown as well as the limits obtained by dark matter detector experiments and the Tokyo Helioscope. At low mass, 10<sup>-5</sup> eV, these microwave cavity experiments are the most sensitive.

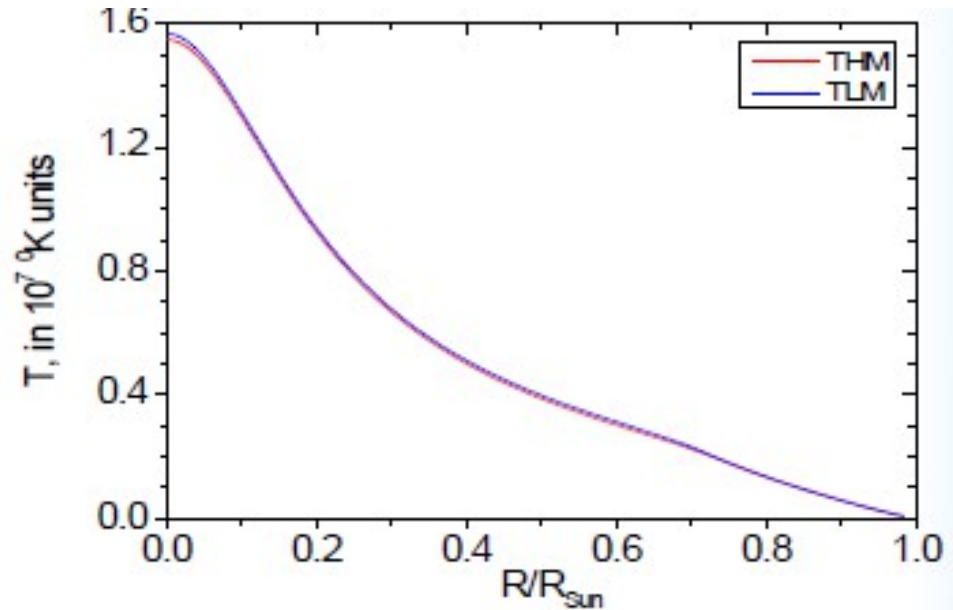
[http://irfu.cea.fr/Sap/en/Phoce/Vie\\_des\\_labos/Ast/ast.php?t=fait\\_marquant&id\\_ast=2582](http://irfu.cea.fr/Sap/en/Phoce/Vie_des_labos/Ast/ast.php?t=fait_marquant&id_ast=2582)

# Flux of solar $^{83}\text{Kr}$ axions

The total axion flux  $\Phi_A$  depends on the level energy  $E_\gamma = 9.4\text{keV}$ , temperature  $T$ , nuclear level lifetime  $\tau_\gamma = 3.6\mu\text{s}$ , the abundance of the  $^{83}\text{Kr}$  isotope on the Sun  $N$ , and the branching ratio of axions to photons emission  $\omega_A/\omega_\gamma$ :

$$\Phi_A = \int N(r) \frac{2 \exp(-E_\gamma / kT(r))}{1 + 2 \exp(-E_\gamma / kT(r))} \frac{\omega_A}{\tau_\gamma \omega_\gamma} dr$$

$$\Phi_A(E_{M1}) = 5.97 \times 10^{23} \left( \frac{\omega_A}{\omega_\gamma} \right) \text{cm}^{-2} \text{s}^{-1} \text{keV}^{-1}$$



$$m_a = \frac{\sqrt{z}}{1+z} \frac{f_\pi m_\pi}{f_a} = 1\text{eV} \frac{\sqrt{z}}{1+z} \frac{1.3 \cdot 10^7}{f_a/\text{GeV}}$$

where  $m_\pi$  и  $f_\pi$  – mass and decay constant of neutral pion,  $z = m_u/m_d = 0.56$  – quark mass ratios.  
 $f_\pi \cong 93 \text{ MeV}$ .

# Resonant absorption by $^{83}\text{Kr}$ nucleus

$$\sigma(E_A) = 2\sqrt{\pi}\sigma_{0\gamma}\exp\left[\frac{-4(E_A - E_{M1})}{\Gamma^2}\right]\frac{\omega_A}{\omega_\gamma}$$

$$\frac{\omega_A}{\omega_\gamma} = \frac{1}{2\pi\alpha} \frac{1}{1+\delta^2} \left[ \frac{g_{AN}^0\beta + g_{AN}^3\beta}{(\mu_0 - 0.5)\beta + \mu_3 - \eta} \right]^2 \left( \frac{p_A}{p_\gamma} \right)^3$$

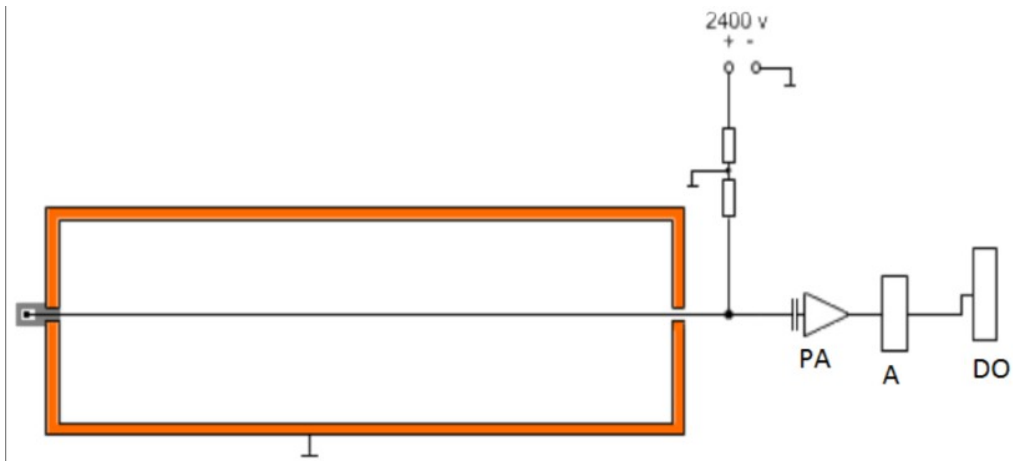
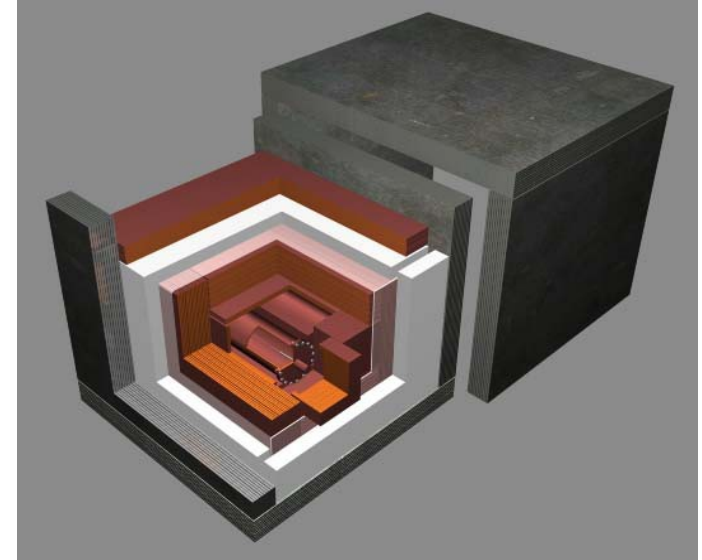
where  $\delta$  – quenching factor for M1 transition,  $\alpha \approx 1/137$ ,  $\mu_0 \approx 0.88$  and  $\mu_3 \approx 4.71$  – isoscalar and izovector nuclear magnetic moments,  $\beta = -1$  and  $\eta = 0.5$  – nuclear matrix constants.

$$g_{AN}^0 = -7.8 \cdot 10^{-8} \left( \frac{6.2 \cdot 10^6}{f_a / \text{GeV}} \right) \left( \frac{3F - D + 2S}{3} \right) \quad g_{AN}^3 = -7.8 \cdot 10^{-8} \left( \frac{6.2 \cdot 10^6}{f_a / \text{GeV}} \right) \left( (D + F) \frac{1 - z}{1 + z} \right)$$

$$\begin{aligned} R[g^{-1} \text{day}^{-1}] &= 4.23 \times 10^{21} \left( \frac{\omega_A}{\omega_\gamma} \right)^2 = \\ &= 8.53 \times 10^{21} (g_{AN}^3 - g_{AN}^0)^4 \left( \frac{p_A}{p_\gamma} \right)^6 = \\ &= 2.41 \times 10^{-10} m_A^4 \left( \frac{p_A}{p_\gamma} \right)^6 \end{aligned}$$

# Experimental Setup

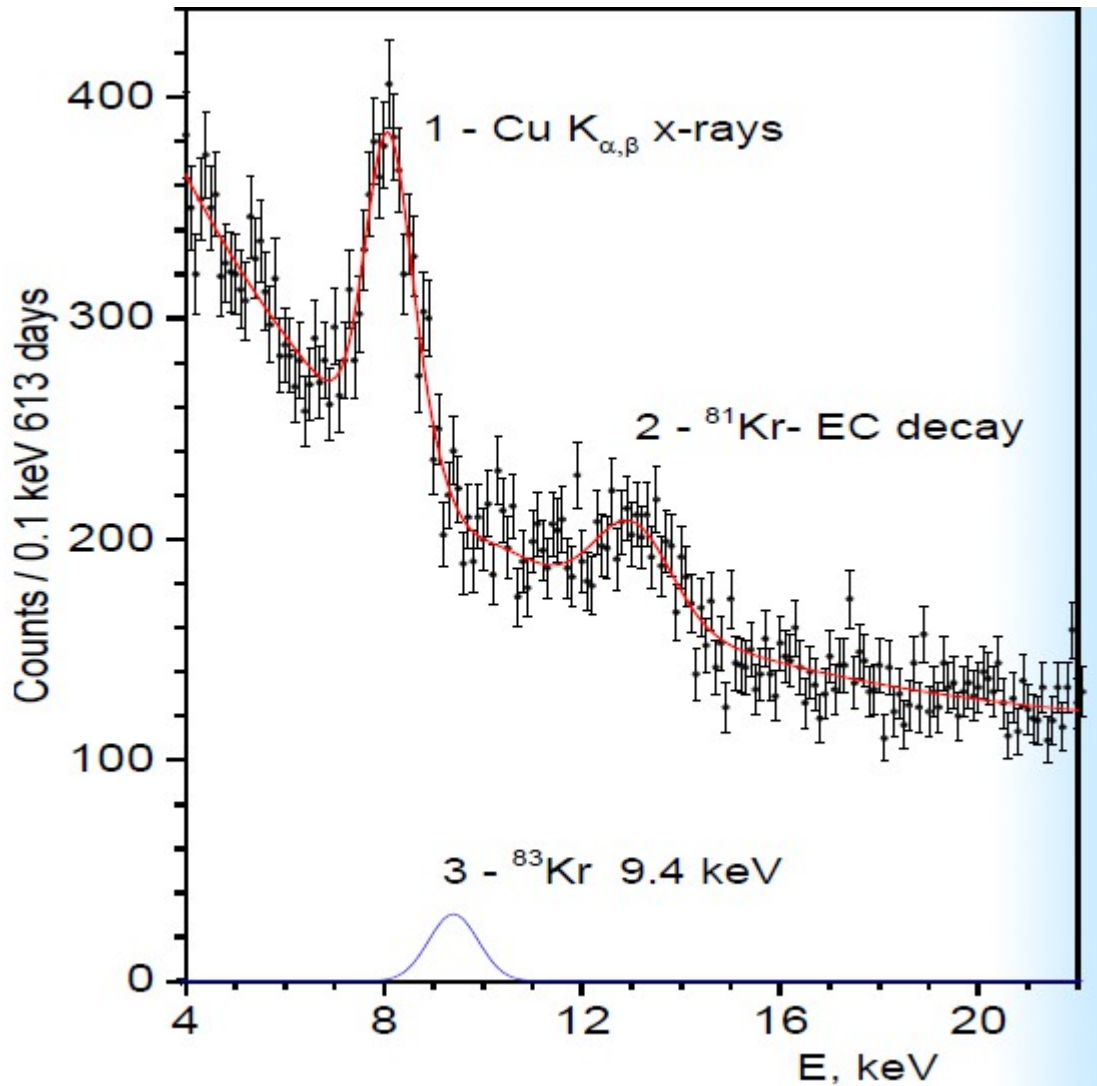
Detector	Proportional counter
Shield	23cm Pb, 8cm PE, 20cm Cu
Working gas	99.9% Kr-93
Diameter (case)	134 mm
Anode (gold coated tungsten)	10 $\mu\text{m}$
Fidutial length	595 mm
Gas pressure	1.8 at



**PA – Preamplifier**  
**A1 – Amplifier**  
**DO – FADC (Digitizer)**

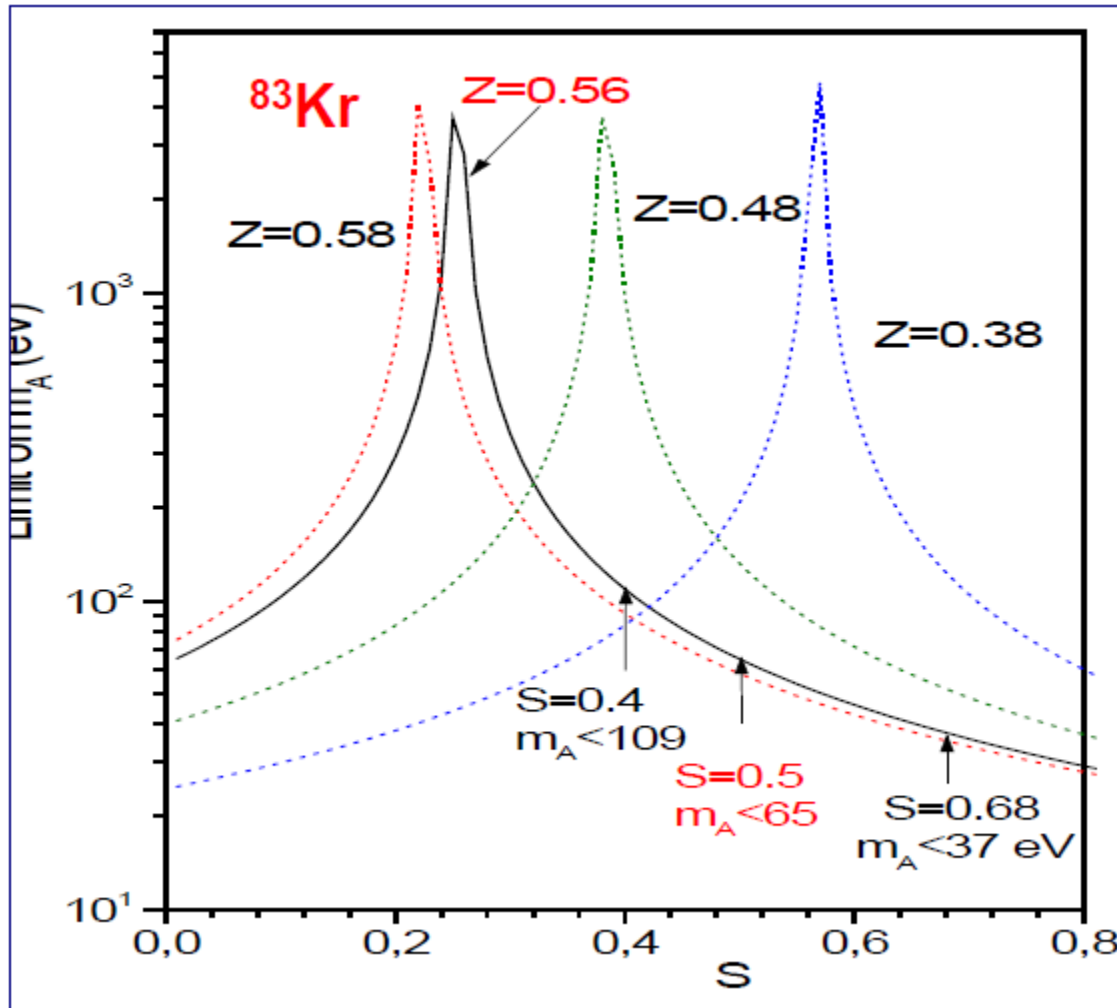


# Phase II – 613 days spectrum of 99% $^{83}\text{Kr}$ -detector



Spectra of Kr-chamber measured during 613 days of livetime. The peak of 13.5keV from K-capture of  $^{81}\text{Kr}$  is in  $1.2 \times 10^3$  times less intensive than Phase I results. Since the proportional chamber is prepared from copper and Cu X-rays are clear visible.

# Results:



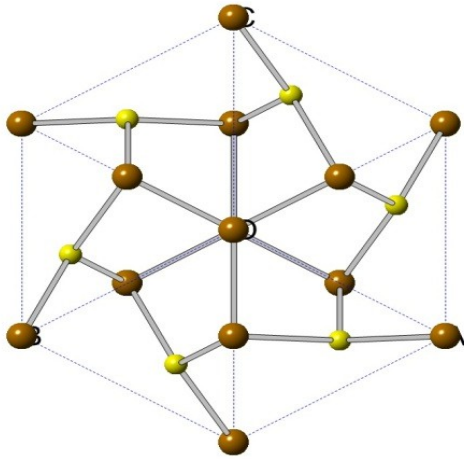
$$|\lg^3_{AN} - g^0_{AN}| \leq 8.4 \times 10^{-7},$$
$$m_A \leq 65 \text{ eV at 95\% C.L.}$$

Nuclide	Abundance in heliosphere, $\log_{10}s$ ( $\log_{10}s(\text{H})=12.00$ )	1-st excitation level, keV (transition type)
Fe-57	5,78	14,41 (M1+E2)
Kr-83	2,34	9,40 (M1+E2)
Li-7	0,42	477,6 (M1+E2)

## Overview of other experimental results

	Article (nuclide)	Результат
1	M. Krcmar et al., arXive:nucl-ex/9801005v2 (Fe-57)	$\leq 745$ eV
2	K. Jakovčić et al., arXive:nucl-ex/0402016v1 (Kr-83)	$\leq 5,5$ keV
3	A.V. Derbin et al., Eur. Phys. J. C (2009) 62:755-760 (Fe-57)	$\leq 159$ eV
4	F.A. Danevich et al., arXive:nucl-ex/0811383v2 (Fe-57)	$\leq 1,6$ keV
5	P. Belli et al., Nucl. Phys. A (2008) 806:388-397 (Li-7)	$\leq 13,9$ keV
6	Yu.M. Gavriljuk, et al., JETP Letters (2015,) (Kr-83)	$\leq 99,5$ eV
7	<b><i>This work (Kr-83)</i></b>	<b><math>\leq 65</math> eV</b>
	W.C. Haxton and K.Y. Lee, Phys. Rev. Lett. (1991)	$\approx 3 \div 20$ eV

# Pyrite



The mineral pyrite, or iron pyrite, also known as fool's gold, is an iron sulfide with the chemical formula  $\text{FeS}_2$ . Pyrite has been proposed as an abundant, inexpensive material in low-cost photovoltaic solar panels. Synthetic iron sulfide was used with copper sulfide to create the photovoltaic material.



The band gap in pyrite is about 0.95 eV and the dominant charge carriers can be either electrons or holes. Sometimes, both n-type and p-type semiconducting regions can be found within single naturally occurring crystals

Single crystal has a cubic form.

Resistivity (natural crystals):  $10^{-5} \div 10^0 \text{ Ohm} \cdot \text{m}$

# New detector for Solar hadronic axions

**Detector:** semiconductor detector based on Pyrite or other crystal containing  $^{57}\text{Fe}$

**Hall mobility:**  $0.5 \div 3 \text{ cm}^2/\text{V}\cdot\text{s}$

**Electron mobility:**  $10 \div 50 \text{ cm}^2/\text{V}\cdot\text{s}$

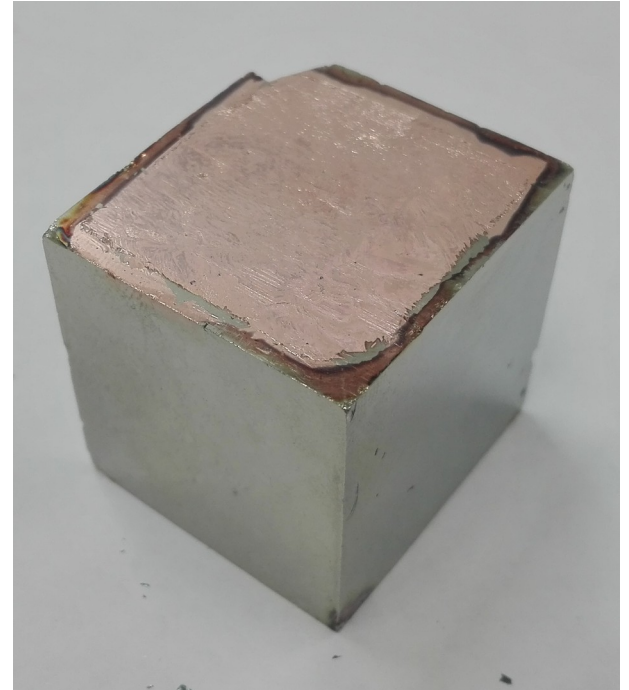
**Isotope abundance:**  $^{54}\text{Fe}$ -5,845%,  $^{56}\text{Fe}$ -91,754%,

$^{57}\text{Fe}$ -2,119%,  $^{58}\text{Fe}$ -0,282%

$$R [g^{-1} day^{-1}] = 8.48 \times 10^{-7} m_A^4 \left( \frac{P_A}{P_Y} \right)^6$$

$$\frac{R_{Fe-57}}{R_{Kr-83}} = 3.51 \times 10^3$$

$$\text{goal: } S(m_A) \simeq 1 eV$$



## We have:

1. 3 natural Pyrite crystals from market (~3cm side).
2. Cryostat (-196 ÷ +500 °C).

## Our plans:

1. Manufacturing natural crystals to produce Diodes.
2. Producing synthetic crystals:  $\text{GaS:Fe}$ ,  $\text{Ga}_2\text{S}_3:\text{Fe}$ ,  $\text{FeS}_2$

## Main goal:

Development a detector of axions made of one of above sined crystals.

# «Blue photoluminescence of $\alpha$ -Ga<sub>2</sub>S<sub>3</sub> and $\alpha$ -Ga<sub>2</sub>S<sub>3</sub>:Fe<sup>2+</sup> single crystals»

Chang-Sun Yoon, F. D. Medina, L. Martinez, et al.,  
Appl. Phys. Lett. 83, 1947 (2003); doi: <http://dx.doi.org/10.1063/1.1609254>

## ABSTRACT:

$\alpha$ -Ga<sub>2</sub>S<sub>0</sub> and  $\alpha$ -Ga<sub>2</sub>S<sub>3</sub>:Fe<sup>2+</sup> single crystals were grown by the two-zone sublimation method. The optical energy gaps of  $\alpha$ -Ga<sub>2</sub>S<sub>0</sub> and  $\alpha$ -Ga<sub>2</sub>S<sub>3</sub>:Fe<sup>2+</sup> at 10 K were found to be 3.440 and 3.392 eV, respectively. From the absorption spectra of  $\alpha$ -Ga<sub>2</sub>S<sub>3</sub>:Fe<sup>2+</sup>, the crystal field parameter Dq of 345 cm<sup>-1</sup> and Racah parameters B of 700 and C of 3365 cm<sup>-1</sup> were obtained for tetrahedral Fe<sup>2+</sup> ions. From the photoluminescence spectra at 10 K, the blue and red emissions at 424 and 643 nm, respectively, for  $\alpha$ -Ga<sub>2</sub>S<sub>0</sub> and the violet and yellow emissions at 400 and 580 nm, respectively, for  $\alpha$ -Ga<sub>2</sub>S<sub>3</sub>:Fe<sup>2+</sup> were observed. All the emission lines observed in the photoluminescence spectra were identified.

# Pyrite single crystal in cryostat LN-120 (Cryotrade)





**Thanks!**